First principles calculation of elastic properties of $AlMgB_{14}$

Yongbin Lee and B. N. Harmon

Ames Laboratory and Department of Physics and Astronomy, Iowa State University, Ames, Iowa 50011

(August 22, 2002)

Abstract

We have calculated the electronic structure and elastic properties of $AlMgB_{14}$ for which, with small chemical modification, ultra hardness was reported recently. The calculated density of states and elastic constants are presented. Additionally, we have calculated the elastic anisotropy and elastic wave velocity. Together with the measured hardness, the calculated shear modulus is consistent with the empirical proportionality observed between shear moduli and microhardness.

PACS No.: 62.20.Dc,62.20.Qp,71.20.Lp

I. INTRODUCTION

After their discovery[1], boron rich compounds that consist of B_{12} icosahedra have been the subject of numerous investigations because of their novel scientific properties and potential technical applications. Their common properties originate from B_{12} icosahedra while their individual character is determined by interstitial atoms. A common characteristic is the refractory nature of boride compounds[2], and many practical applications of boron-rich compounds are related to this property - with uses in the field of nuclear energy, aerospace and the military.[3] Recently, Ames Laboratory scientists discovered an interesting mechanical property for $AlMgB_{14}$. Its hardness reached that of the second hardest material, cubic BN(c-BN) with small chemical additions - TiB_2 addition gives 35 - 46 GP hardness and Si gives 32 - 37 GPa.[4] This observation is very intriguing because $AlMgB_{14}$ is far from the conventional paradigm for ultrahard materials, lacking the usual high symmetry, small unit cell, and small bond lengths. Scientifically it might provide a good example to investigate how hardness can be enhanced by microstructural complexity and chemical doping. It may also prove very useful because it may replace the expensive c-BN for technical applications.

The structure of $AlMgB_{14}$ had been reported by Matkovich and Economy[5] and after that there have been several additional publications about its crystal structure[6–8], optical and electric properties.[9,10] Most of these studies were experimental. Although electronic structure investigations are very important for understanding material properties, the complexity of this material is quite formidable even for modern computational methods, and to our knowledge no previous calculations have been reported. $AlMgB_{14}$ has the orthorhombic structure with lattice constants a=0.5848 nm, b=1.0312 nm, c=0.8112 nm , space group *Imma*, and 4 formula units per cell. Additionally, it has vacancies(2 per cell) at the metal sites. With new parallelized computational band structure techniques[11] we have been able to investigate the electronic structure for this complex material and have calculated its elastic constants.

II. ELASTIC CONSTANTS, RESULTS

Elastic constants are believed to be related to the strength of materials. Especially, the bulk and shear moduli are frequently calculated for materials when investigating their hardness. The bulk modulus calculation for a single crystal is easier than the shear modulus calculation because hydrostatic pressure does not change the crystal symmetry. However the correlation between material hardness and shear modulus exhibits better consistency than for the bulk modulus.[12] Furthermore, the whole set of elastic stiffness constants(ESCs), or elastic compliance constants(ECCs), have to be calculated to extract the theoretical polycrystalline bulk modulus and shear modulus. And, because the number of these constants increases as the crystal symmetry decreases, the polycrystalline bulk and shear modulus calculations for low symmetry materials can be computationally demanding.

The elastic strain tensor ε_{ij} is related to the stress σ_{ij} by Hooke's law

$$\sigma_{ij} = \sum_{k,l=1}^{3} c_{ijkl}\varepsilon_{kl} \tag{1}$$

Using Voigt's contraction[13], this is usually written as :

$$\sigma_{\alpha} = \sum_{\beta=1}^{6} c_{\alpha\beta}\varepsilon_{\beta} \tag{2}$$

where

$$\sigma_{\alpha} = \sigma_{ij},$$

$$\varepsilon_{\beta} = \varepsilon_{kl} \text{ if } \beta = 1,2 \text{ or } 3$$

$$\varepsilon_{\beta} = 2\varepsilon_{kl} \text{ if } \beta = 4,5 \text{ or } 6$$

The number of independent components of the ESC tensor $c_{\alpha\beta}$ depends on crystal symmetry. This number is 3 for a cubic material, 5 for a hexagonal one, 9 for an orthorhombic one, and 21 for a triclinic material.[13]

There are two approximations used to calculate the extreme bulk and shear modulus for a statistically isotropic polycrystalline single phase material - the Voigt method and

the Reuss method.[13] The first one assumes a uniform strain and gives the bulk(K_V) and shear(G_V) moduli as functions of the ESCs.

$$K_V = \frac{1}{9}(c_{11} + c_{22} + c_{33}) + \frac{2}{9}(c_{12} + c_{23} + c_{13}) \tag{3}$$

$$G_V = \frac{1}{15}(c_{11} + c_{22} + c_{33}) - \frac{1}{15}(c_{12} + c_{13} + c_{23}) + \frac{1}{5}(c_{44} + c_{55} + c_{66}) \tag{4}$$

The second one assumes a uniform stress and gives K and G as function of the ECCs.

$$\frac{1}{K_R} = (s_{11} + s_{22} + s_{33}) + 2(s_{12} + s_{23} + s_{13}) \tag{5}$$

$$\frac{1}{G_V} = \frac{4}{15}(s_{11} + s_{22} + s_{33}) - \frac{4}{15}(s_{12} + s_{13} + s_{23}) + \frac{3}{15}(s_{44} + s_{55} + s_{66}) \tag{6}$$

If they are applied to calculate average isotropic elastic moduli for polycrystalline samples using the anisotropic single crystal elastic constants, they give the theoretical maximum (Voigt method) and minimum (Reuss method) values of isotropic elastic moduli.[14] Frequently, their arithmetic averages $K = (K_V + K_R)/2$, $G = (G_V + G_R)/2$ are taken for an estimation of the elastic properties. The other two elastic constants describing an isotropic polycrystalline material, the Young modulus(E) and the Poisson ratio(ν), can be expressed as

$$E = \frac{9KG}{3K + G} \tag{7}$$

$$\nu = \frac{3K - 2G}{2(3K + G)} \tag{8}$$

Additionally, we remark that the limiting values of the Voigt and Reuss approximations are the same for a polycrystalline sample of isotropic crystallites, but a difference is expected for an aggregate of anisotropic crystallites. The magnitude of the difference is a function only of the degree of elastic anistropy possessed by the crystal under consideration. Therefore, it is useful to evaluate the percent of elastic anisotropy of materials.[14] For bulk(A_K) and shear(A_G), this can be defined as

$$A_K = \frac{K_V - K_R}{K_V + K_R} \tag{9}$$

$$A_G = \frac{G_V - G_R}{G_V + G_R} \tag{10}$$

The elastic anisotropy of materials is a primary cause for detrimental microcracks that are induced in ceramics.[15,16]

Because the ESC tensor **c** is related to the ECC tensor **s** by

$$\mathbf{cs} = \mathbf{I}_6$$

the polycrystalline elastic moduli for both approximations can be calculated by knowing either tensor. We calculated all of the ESCs for $AlMgB_{14}$. After choosing the strain components corresponding to each ESC, we established 9 corresponding distortion matrices **D**.[16] With different values of the distortion parameter, these symmetric distortion matrices transformed the original lattice vector set to new distorted lattice vector sets $\mathbf{R}' = \mathbf{RD}$. We calculated the total energies of these distorted crystal structures for several different distortion magnitudes. ESCs are estimated from the total energies. Actually, the ESCs are given by the second order coefficients in the polynomial fit of the total energy versus the distortion parameter.[17] For a more detailed explanation of the distortion matrix, the reader is refered to Ref. 16.

We used the parallelized full-potential, linear augmented plane method[11] within the local-density approximation with the Hedin-Lindqvist[18] exchange-correlation potential. Most of these calculations were performed using the SP machine at NERSC. We iterated with the equivalent of 64 **k**-points in the whole Brillouin zone to calculate self-consistent total energies. The number of augmented plane waves for these calculations was about 3500. The muffin-tin radius is 1.5 a.u. for B atoms, 2.2 a.u. for Al atoms and 2.7 a.u. for Mg atoms. The value of the plane-wave cutoff KR_{max}= 6 was determined by the radius of the B atoms because they have a much smaller muffin-tin radius than the metal atoms. We calculated both the 64 atoms per cell case and the 62 atoms per cell case, which has two vacancies at the metal

sites.[5,7]. As shown in Fig.1, one vacancy is at the Al site (0.0, 0.5, 0.0) and another is at the Mg site (0.75, 0.5, 0.391)

Calculations for the full 64 atoms per cell structure show that the Fermi level lies in states above a band gap of about 1eV. With the observed 25% vacancies on the Al and Mg sites, calculations indicate that the Fermi level falls below the gap, near the top of a broad set of bands having predominately boron charater(see Fig.2). The vacancies lower the total energy per atom below that of the 64 atoms per cell structure. For the 62 atoms case, the top most valence band is half full (one hole per unit cell), and thus the ideal ordered structure should be metallic. With disordered vacancies, the scattering of electrons near the top of the occupied boron bands at the Fermi level can be very high and some of the electronic states could become localized. One would thus expect transport properties such as electrical resistivity to be sensitive to sample preparation methods since processing parameters such as cooling rate will determine the degree of ordering of the vacancies and induce other microstructural defects affecting scattering. It is also possible that the vacancies could cluster locally (e.g. near defects or grain boundaries) and thus affect the local electronic structure, causing some parts to be ceramic like and others parts to have some degree of metallic behavior. Chemically doping the sample, for example with Si, would add electrons to the valence band. It is expected that when the valence bands are completely filled and the Fermi level lies within the gap, the material will have maximum resistivity, and properties may change rapidly as the nature of the electronic states at the Fermi level change quickly with doping. Fig.3 shows the DOS for the sample which has one Si atom at a Al site and two vacancies at metal sites. The Fermi level lies in the gap. There are Si impurity states in the original 1eV gap.

With vacancies, the positions of atoms surrounding each vacancy are slightly shifted from the ideal lattice coordinates. The new relaxed position can be ascertained using total force calculations.[19,20] Although this results in lower total energy, it is well known that atomic position relaxation usually gives smaller elastic constants than for the unrelaxed case.[21] Fig.4 is the density of states(DOS) for the 62 atoms per cell case with optimized atomic positions.

For this calculation, the 62 atoms are relaxed until the force components exerted on each atom are decreased to less than 0.014(eV/Å). Compared with the unrelaxed case, the total energy is lower and the DOS is decreased near the Fermi level(see Fig.2). Although the relaxed structure is more stable than the unrelaxed one, preliminary calculations for relaxed $AlMgB_{14}$ shows that the elastic constants do not change much in the optimized case.

Table I shows the ESC obtained by polynominal fits to the total energy and Table II gives the elastic properties calculated by Eq(3) - Eq(8) for both the 64 and 62 atom cases. Included in Table II are the two extreme values (Voigt and Reuss), and the average. Most of the constants are slightly decreased with the presence of vacancies. The calculated bulk and shear moduli are not as big as those for superhard materials, which is to be expected for $AlMgB_{14}$, because the superhardness of $AlMgB_{14}$ compounds is attained only by chemical and microstructural modification. The measured Vickers hardness of $AlMgB_{14}$ is 27-28 GPa for a single crystal[8] and 32-35 GPa for a polycrystalline sample.[4] The calculated value of the shear modulus of $AlMgB_{14}$ (215 GPa) is similar with those of B_6O (204 GPa), rutile-SiO_2 (220 GPa), and SiC (196 GPa). The corresponding microhardnesses are 35, 33, 29 GPa. $AlMgB_{14}$ has a reasonable position on the shear modulus *vs* hardness plot(Fig.5).[12] Another interesting quantity given in Table II is the Poisson ratio. This has been used to charaterize bonding, with $\nu = 0.25$ suggested as the low limit for a central force solid.[16] The low Poisson ratio of $AlMgB_{14}$ and the large value of the ratio of the shear modulus to bulk modulus (G/K=1.13) suggest that this material has noncentral, directional covalent bonds.[22]

Table III shows the calculated anisotropy and elastic wave velocity in $AlMgB_{14}$, with the assumption that this material is isotropic polycrystalline. The relationships between the sound wave velocity and the elastic constants are

$$C_L = \left[\frac{K + (4/3)G}{\rho}\right]^{1/2} \tag{11}$$

$$C_T = \left[\frac{G}{\rho}\right]^{1/2} \tag{12}$$

and their average is

$$C_M = \left[\frac{1}{3}\left(\frac{2}{C_T^3} + \frac{1}{C_L^3}\right)\right]^{-1/3} \tag{13}$$

The transverse modes are degenerate in isotropic polycrystalline materials.[13] One interesting observation is that the sound wave velocity approaches that of diamond's. Even though there are vacancies, $AlMgB_{14}$ has nearly isotropic elastic properties. It might be explained by the consideration of the role of icosahedra in boron-rich solids. The nearly isotropic elastic properties of boron rich solids could be a common character that might be attributed to the iscosahedra skelton. The icosahedra are centered at (0.25, 0.25, 0.25), (0.25, 0.75, 0.25), (0.75, 0.25, 0.75) and (0.75, 0.75, 0.75) in $AlMgB_{14}$ and are highly symmetric(see Fig.1).

In summary, we have calculated elastic properties - elastic constants, elastic anisotropy and elastic wave velocities for $AlMgB_{14}$. The elastic moduli and the measured microhardness are consistent with other hard materials, but there is little that can be directly related to the dramatic increase in hardness caused by Si doping. The microstructure of these chemically modified samples needs to be investigated. Experiments of optical properties and even electrical conductivity would help elucidate the electronic structure and the possible role of defects and doping.

ACKNOWLEDGMENTS

The Ames Laboratory is operated for the U. S. Department of Energy by Iowa State University under Contract No. W-7405-Eng-82. We thank to Dr. B. Cook and Professor A. Russell for their helpful discussions and comments. We also thank Professor Art Freeman, Dr. Miyoung Kim, and Dr. Andrew Canning for advice on using the parallelized FLAPW program. The calculations were performed using the supercomputing facilities at the National Energy Research Scientific Computing Center(NERSC).

REFERENCES

[1] G. S. Zhdanov and N. G. Sevastyanov, Compt. rend. Acad.Sci. USSR, **32** ,432 (1941)

[2] David Emin, Mat. Res. Soc. Symp. Proc. Vol 97, 3 (1987)

[3] R. Telle, L. S. Sigl, and K. Takagi, Handbook of Ceramic Hard Materials (WILEY-VCH, New York, 2000) vol.2, 803

[4] B. A. Cook, J. L. Harringa, T. L. Lewis, and A. M. Russell, Scr. Mater., **42(6)**, 597 (2000)

[5] V. I. Matkovich and J. Economy, J.Acta Cryst., **26**, 616 (1970)

[6] R. Naslain, A. Guette and P. Hagenmuller, Journal of the Less-Common Metals, **47**, 1 (1976)

[7] Iwami Higashi and Tetsuzo Ito, Journal of the Less-Common Metals, **92**, 239 (1983)

[8] Iwami Higashi *et. al.*, Journal of Crystal Growth , **128**, 1113 (1993)

[9] Helmut Werheit *et. al.*, Journal of Alloys and Compound, **202** , 269 (1993)

[10] I. A. Bairamashvili *et. al.*, Journal of the Less-Common Metals, **67**, 461 (1979)

[11] A. Canning, W. Mannstadt, A. J. Freeman, Computer Physics Communications, **130**, 233 (2000)

[12] David M. Teter, MRS Bulletin, **23**, 22 (1998)

[13] G. Grimval, Thermophysical properties of materials (North-Holland Physics Publishing, Amsterdam 1986)

[14] D. H. Chung, W. R. Buessem, Anisotropy in single crystal refractory compound (Plenum Press, New York, 1968) vol.2, 217

[15] V. Tvergaard and J. W. Hutchinson, J. Am. Chem. Soc. **71**, 157 (1988)

[16] P. Ravindran *et. al.*, J. Appl. Phys., **84**, 4891 (1998)

[17] D. C. Wallace, Thermodynamis of Crystals(Wiley, NEW York, 1972)

[18] L. Hedin and B. I. Lundqvist, J. Phys. C, **4**, 2064 (1971)

[19] P. Pulay, Mol. Phys. **17**, 197 (1969)

[20] R. Yu, D. Singh, and H. Krakauer, Phys. Rev. B **43**, 6411 (1991)

[21] H. W. Hugosson, A theoretical treatise on the electronic structure of designer hard materials(Ph. D. Thesis, unpublished, Uppsala, 2001)

[22] J. Haines *et. al.*, Annu. Rev. Mater. Res., **31**, 1 (2001)

FIGURES

FIG. 1. Crystal structure of $AlMgB_{14}$ with two vacancies at metal sites. The red spheres are Mg atoms, blue are Al atoms, white are vacancy sites and green are boron atoms and icosahedra. The vertical direction is along (0,1,0) and the horizontal direction is along (0,0,1).

FIG. 2. The calculated density of states for $AlMgB_{14}$ with 62 atoms/cell. The Fermi level lies below a band gap of about 1eV and there is one hole per cell. The states below the gap are predominantly due to boron, while the states above the gap are primarily due to Al and Mg.

FIG. 3. The calculated density of states for $AlMgB_{14}$ with Si doping. One Si atom replaces one Al atom with two vacancies at metal sites. The Fermi level lies in the gap. There are Si impurity states in the original 1eV gap.

FIG. 4. The calculated density of states for $AlMgB_{14}$ with relaxed 62 atoms/cell. It shows the decreased number of states near the Fermi level compared to unrelaxed case.

FIG. 5. A plot of microhardness *vs* shear modulus for various materials (see reference 12). The filled circle shows the position of $AlMgB_{14}$.

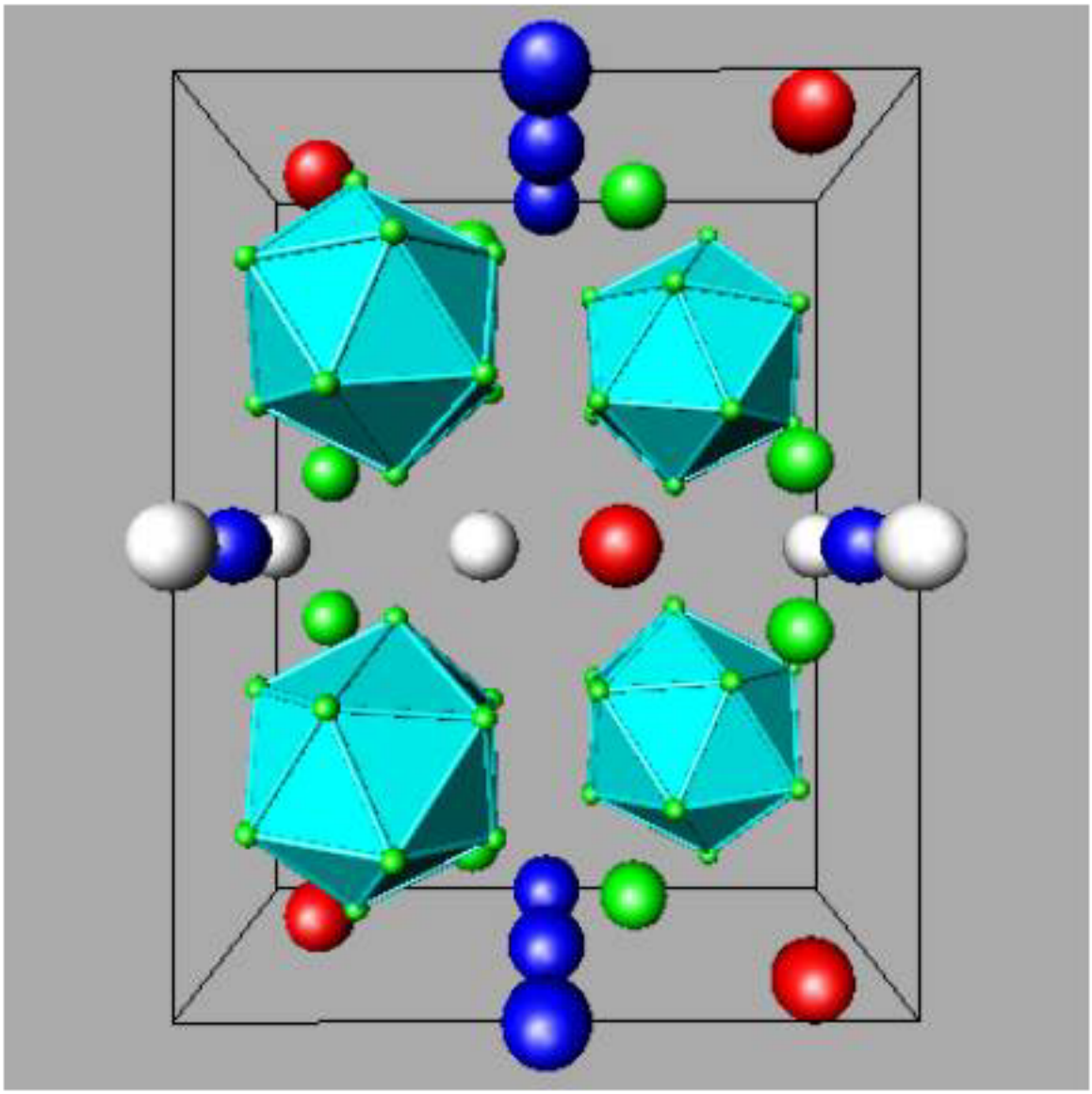

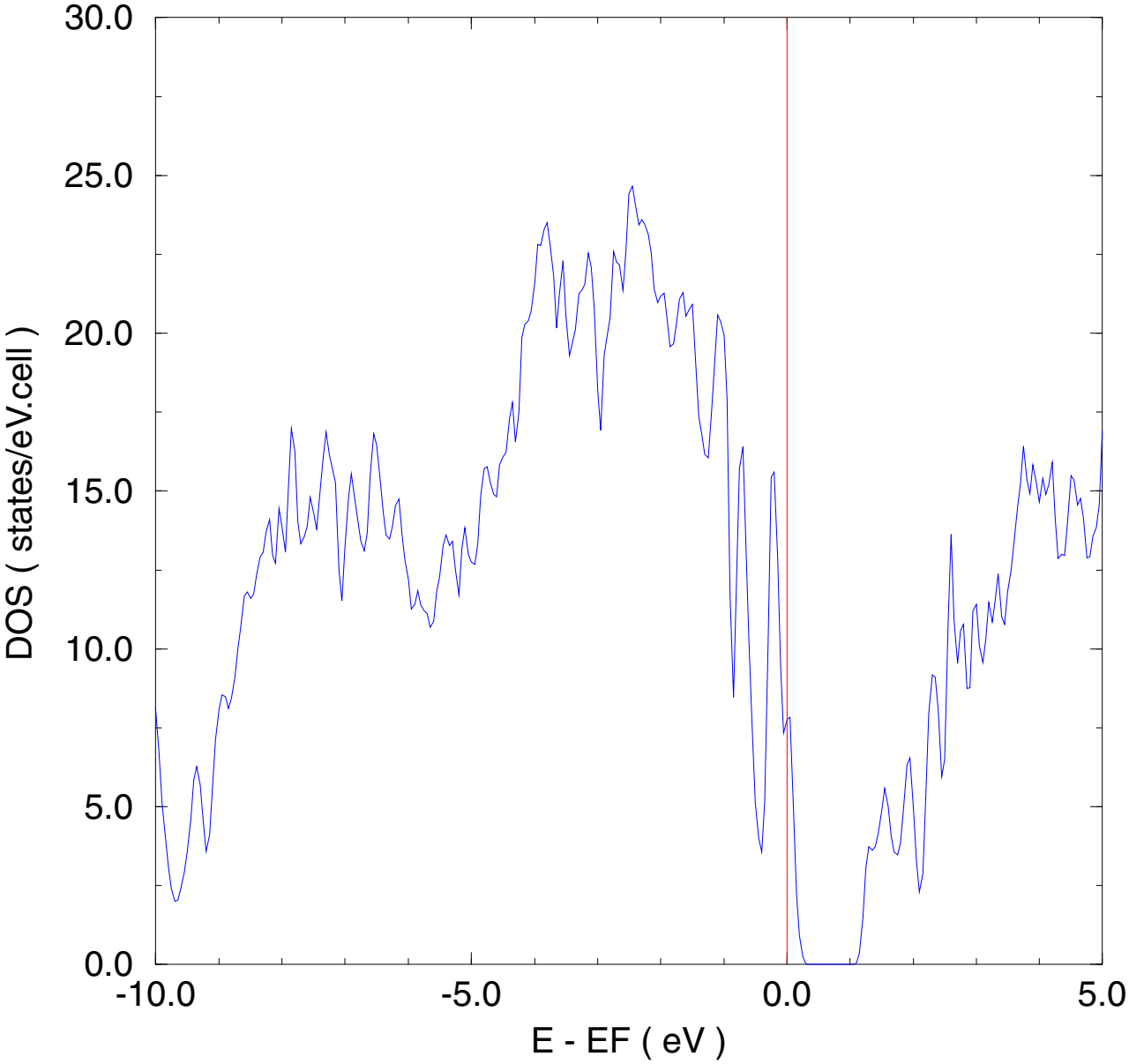
30.0
25.0
20.0
15.0
10.0
5.0
0.0
DOS (states/eV.cell)
-10.0
-5.0
0.0
5.0
E - EF (eV)

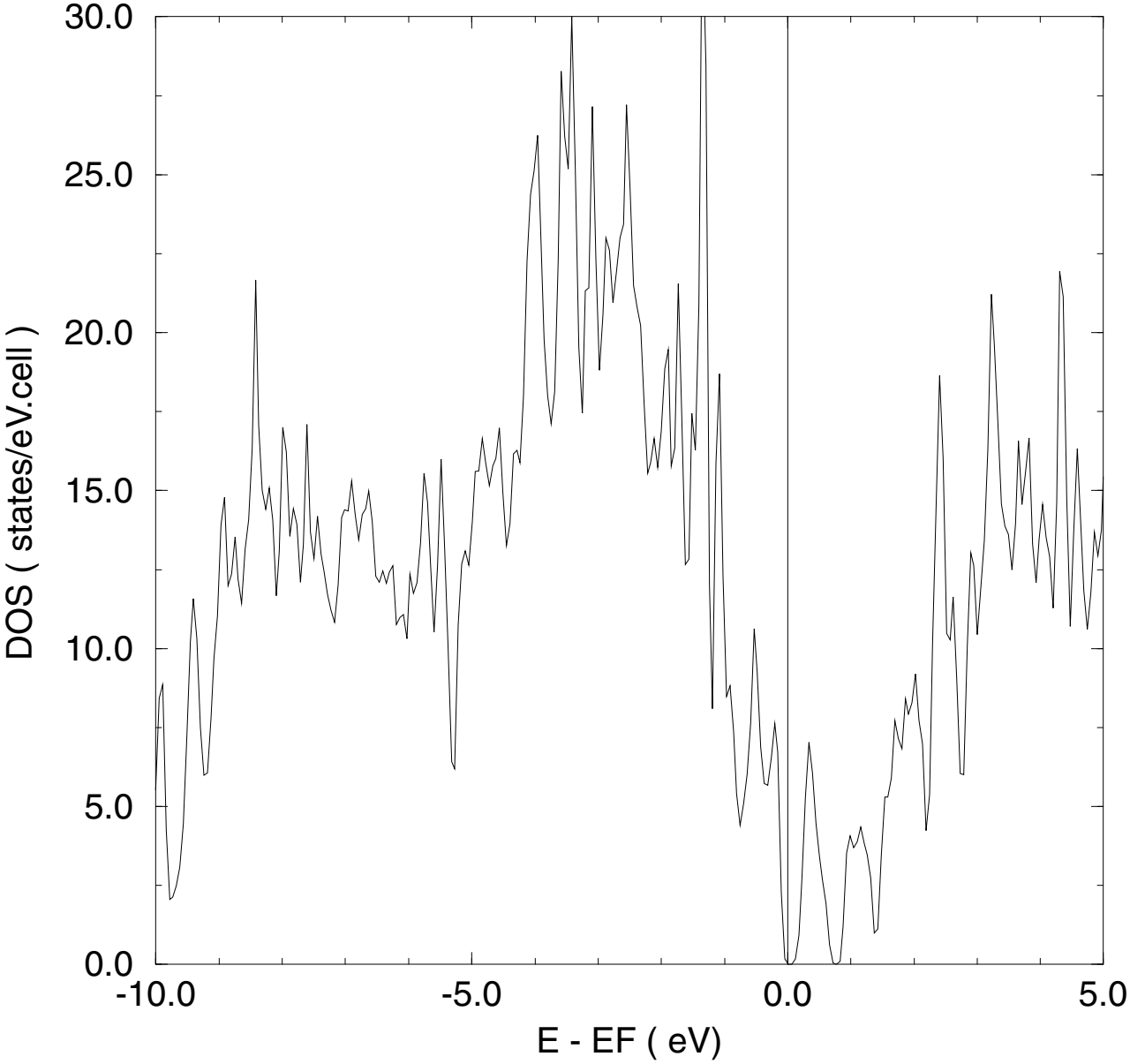
30.0
25.0
20.0
15.0
10.0
5.0
0.0
DOS (states/eV.cell)
-10.0
-5.0
0.0
5.0
E - EF (eV)

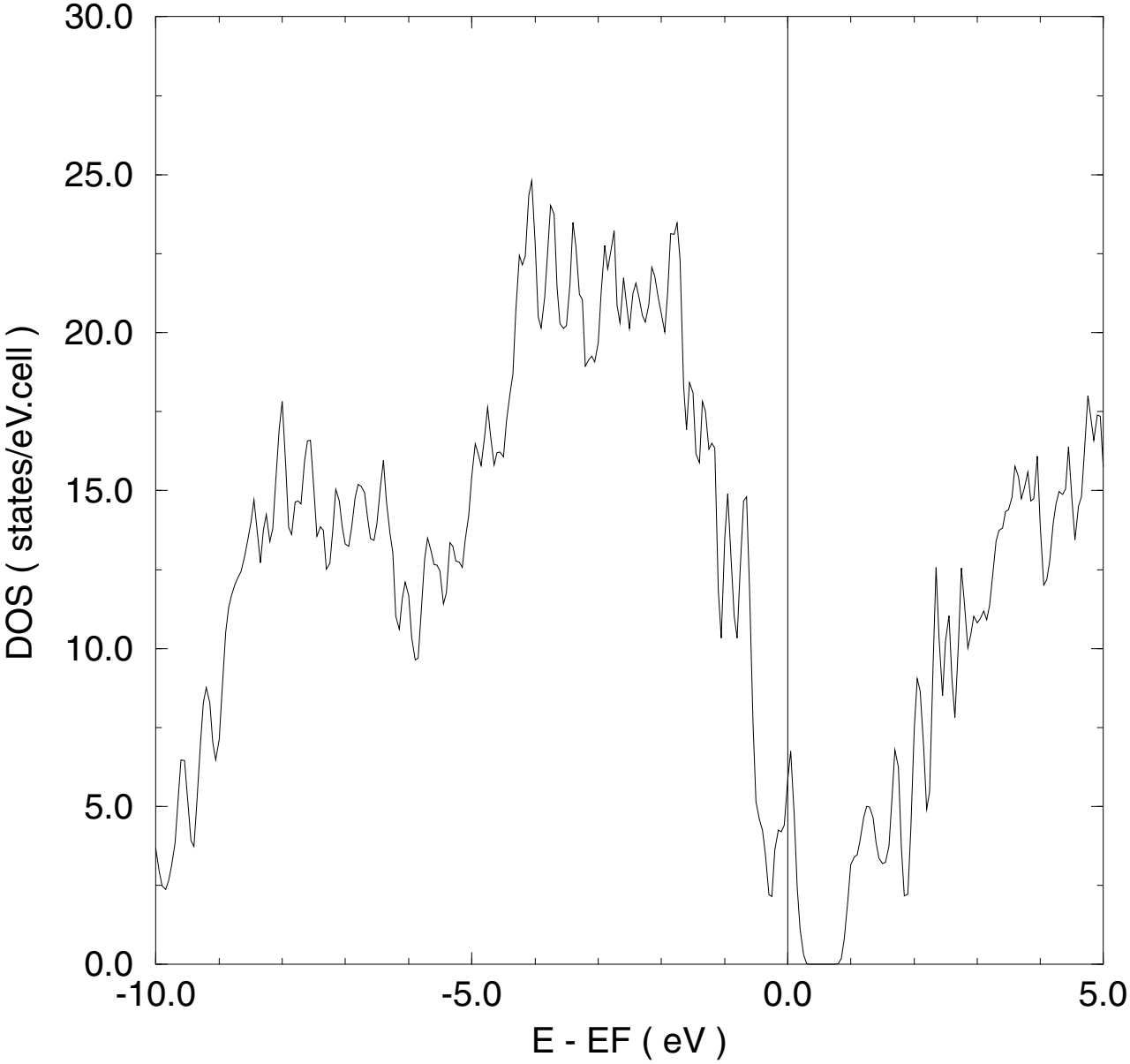
30.0
25.0
20.0
15.0
10.0
5.0
0.0
DOS (states/eV.cell)
-10.0
-5.0
0.0
5.0
E - EF (eV)

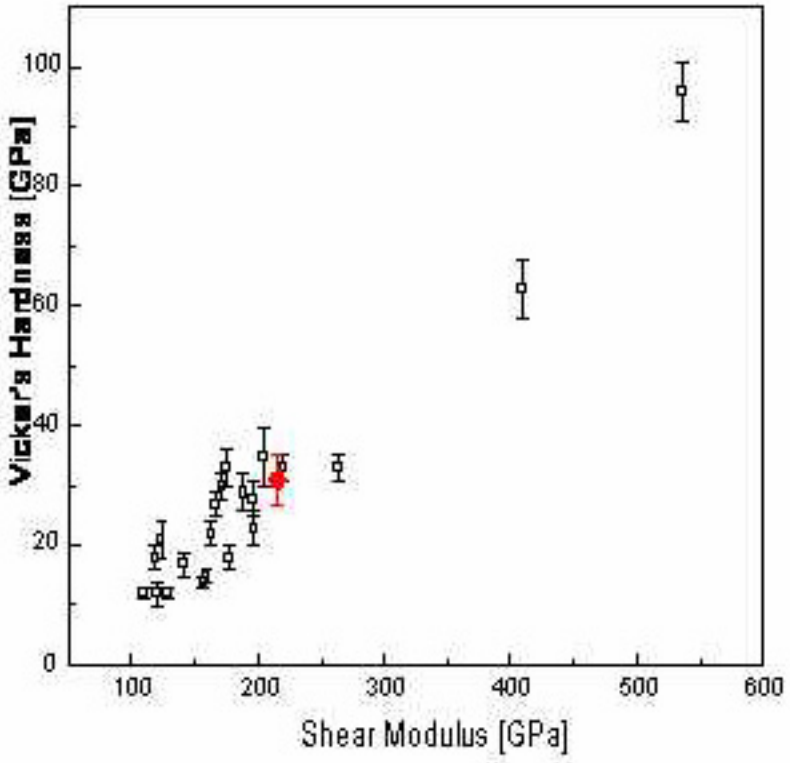
Vicker's Hardness [GPa]
Shear Modulus [GPa]
0
20
40
60
80
100
100
200
300
400
500
600

TABLES

TABLE I. The calculated elastic stiffness constants for both 64 atoms/cell and 62 atoms/cell $AlMgB_{14}$. The numbers within parentheses are fitting errors.

	64 atoms (GPa)	62 atoms (GPa)
c_{11}	545 (1.89)	503 (1.45)
c_{22}	538 (0.81)	500 (1.63)
c_{33}	531 (2.27)	496 (2.86)
c_{44}	199 (0.03)	183 (0.00)
c_{55}	254 (0.67)	252 (0.10)
c_{66}	221 (0.04)	211 (0.06)
$c_{11}+c_{22}-2c_{12}$	1011 (14.93)	936 (11.23)
$c_{11}+c_{33}-2c_{13}$	929 (8.79)	844 (0.78)
$c_{22}+c_{33}-2c_{23}$	988 (16.2)	927 (8.79)
c_{12}	36 (8.82)	33.5 (7.16)
c_{13}	73.5 (6.48)	77.5 (2.55)
c_{23}	40.5 (9.64)	34.5 (6.64)

TABLE II. The elastic properties(bulk modulus (K), shear modulus (G), Young modulus (E), and Poisson ratio (ν)) of polycrystalline $AlMgB_{14}$ calculated with the Voigt and Reuss assumptions. The constants without the subscripts are averages.

	64 atoms	62 atoms
K_V(GPa)	212.67	198.89
K_R(GPa)	212.13	184.03
K(GPa)	212.40	191.46
G_V(GPa)	232.40	219.43
G_R(GPa)	230.12	211.98
G (GPa)	231.26	215.71
E (GPa)	509.04	470.45
ν	0.1	0.09

TABLE III. The percentage anisotropy of bulk(A_K) and shear(A_G) are given along with the calculated longitudinal(C_L), transverse(C_T), and average(C_M) sound velocities. The transverse modes are degenerate in isotropic polycrystaline materials.

	64 atoms	62 atoms
A_K(%)	0.13	3.88
A_G(%)	0.49	1.73
C_L(km/s)	13.8	13.4
C_T(km/s)	9.17	9.01
C_M(km/s)	10.03	9.84